



Magnetic Resonance Imaging and Ultrasound Roles in Evaluation of shoulder impingement syndrome

Mostafa Ali Mohammed Ali Moussa ¹, Awad Abdelaziz Mohammed Bessar ², Hamed Abdelhakiem Mahmoud Gobran², Enas Mahmoud Hamed ²

1 M.B.B.C. Faculty of Medicine – Zagazig University

2 Radiodiagnosis Department, Faculty of Medicine, Zagazig University, Egypt

Email: Mostafaali.ma88@gmail.com

Article History: Received 10th June, Accepted 5th July, published online 10th July 2023

Abstract

Background: While the overall diagnostic sensitivity of the physical exam is reportedly as high as 90%, imaging studies are often performed to confirm the diagnosis of shoulder impingement syndrome and rule out other pathologies. If the decision to obtain radiographs is made, they should be obtained bilaterally, rather than only on the affected side, to evaluate potential anatomic differences and to rule out other pathologies such as calcific tendinitis or arthritic changes. Ultrasonography is particularly useful in assessing the rotator cuff, the subacromial bursa and the long biceps tendon. Ultrasonographic examination must comprehensively cover all shoulder structures that may participate in subacromial disease. In the initial phase of shoulder impingement, swelling compared to the contralateral side may be noted. MRI is the best imaging test prior to arthroscopic surgery. Advantages include the following: Noninvasive, No radiation, Able to detect intrasubstance tendon degeneration or partial rotator cuff tears, Able to detect inflammation, edema, hemorrhage, or scarring, Able to be used with an intra-articular contrast agent (eg, gadolinium), improving the MRI ability to detect partial rotator cuff tears. Disadvantages include the following: Not able to accommodate patients with claustrophobia. Not able to accommodate patients with pacemakers or other metal implants or particles. Dependent on quality of the MRI machine. Dependent on skill of technician performing the imaging and the radiologist interpreting the images and Expensive.

Keywords: Magnetic Resonance Imaging, Ultrasound, shoulder impingement syndrome

DOI: 10.53555/ecb/2023.12.Si12.229

Introduction

While the overall diagnostic sensitivity of the physical exam is reportedly as high as 90%, imaging studies are often performed to confirm the diagnosis and rule out other pathologies. If the decision to obtain radiographs is made, they should be obtained bilaterally, rather than only on the affected side, to evaluate potential anatomic differences and to rule out other pathologies such as calcific tendinitis or arthritic changes (1).

Plain radiograph standard shoulder films include 2 views (AP and lateral/scapular Y) The AP view of the shoulder can be used to determine the critical shoulder angle (CSA), which involves the extent of lateral coverage by the acromion and the inclination of the glenoid. At CSAs greater than 35 degrees, there is an increased likelihood that a rotator cuff is contributing to impingement syndrome. Similarly, measurements such as the acromiohumeral distance (AHD) can help to detect rotator cuff pathologies and defects. The AHD is measured from the inferior edge of the acromion to the humeral head. The normal range is approximately 7 to 14 mm in men and 7 to 12 mm in women. A lower AHD suggests rotator cuff pathology. The scapular Y view allows for the assessment of the humeral head on the glenoid. Additional plain radiographs featuring the outlet view will best visualize and evaluate the shape of the acromion (1).

Other imaging modalities to consider include ultrasound and magnetic resonance imaging (MRI). Consideration for advanced imaging with MRI is recommended after 6 weeks of therapy without clinical improvement. MRI allows for

a detailed evaluation of bony and soft tissue structures within the shoulder girdle. Ultrasound is a bedside imaging option that primarily enables assessment of the soft tissue contributing factors such as bursitis, tendinopathy, and/or tendon ruptures (2).

Ultrasound findings in shoulder impingement syndrome

Ultrasonography is particularly useful in assessing the rotator cuff, the subacromial bursa and the long biceps tendon. Ultrasonographic examination must comprehensively cover all shoulder structures that may participate in subacromial disease. In the initial phase of shoulder impingement, swelling compared to the contralateral side may be noted (3).

Acromioclavicular joint abnormalities:

Degenerative changes and instability in the acromioclavicular joint can cause sub acromial impingement with involvement of the bursa and the supraspinatus tendon. Acromioclavicular osteoarthritis usually affects people over 50 years of age. US can detect distension of the joint capsule, narrowing of the joint space, and marginal osteophytosis of the opposing clavicular and acromial articular surfaces (4).

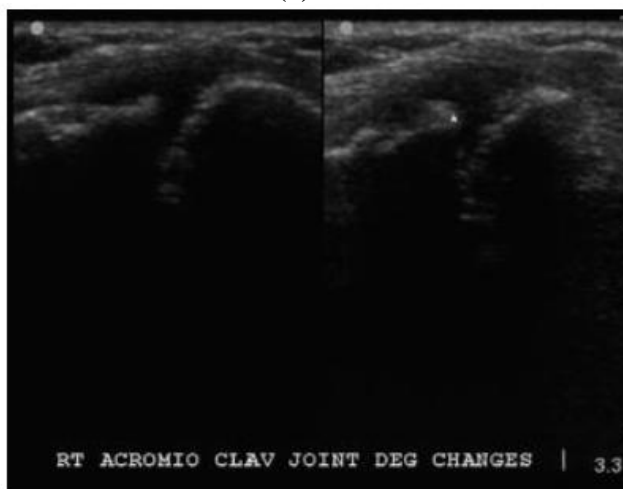


Figure (1): US long axis views of acromioclavicular (AC) joint shows osteophytes (*) and cortical irregularity involving AC joint denoting AC osteoarthritis (4).

Subacromial bursitis:

The subacromial bursa is lined by synovial cells that secrete fluid into it. It is interposed between the echogenic peribursal fat stripe (which is deep to the deltoid) and the superficial margin of the supraspinatus tendon and is generally seen as a thin hypoechoic line, usually less than 2 mm in thickness in normal individuals (5).

The simultaneous presence of bursitis and a superficial lesion on the supraspinatus tendon are suggestive of subacromial impingement. US can demonstrate subacromial bursitis in shoulder impingement by the presence of increased fluid in the bursa and/or thickening of the wall of the bursa, that measures > 2 mm in total. It is important to measure both anechoic effusion and hyperechoic walls (4).

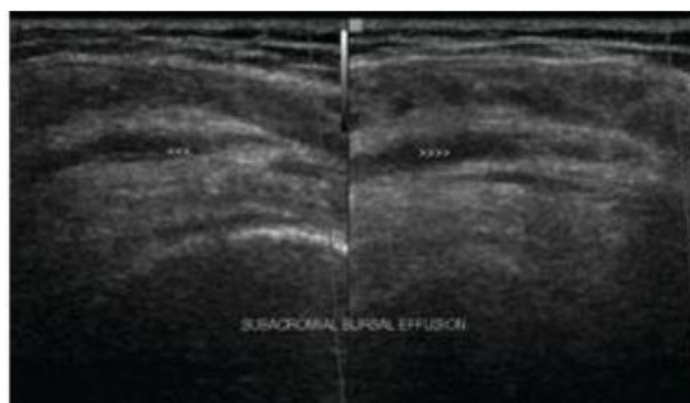


Figure (2): US Long and short-axis views of supraspinatus show anechoic fluid seen distending the subacromial bursa with bursal thickening denoting subacromial bursitis (4).

Abnormalities of the supraspinatus tendon:

A- Sonographic findings of tendinosis:

In degenerative changes of tendons, US can depict irregularities of the fibrillar appearance with focal hypoechoic areas or with diffuse heterogeneous hypo echogenicity. The tendon can appear thickened and irregular, but there are no signs of tendon tear. Hyper vascular pattern of inflammation (hyperemia) and focal calcification could be detected. The tendon may be seen diffusely swollen in acute stages (6)



Figure (3): US image of the supraspinatus tendon, longitudinal view demonstrates loss of the fibrillar pattern of the tendon with diffuse heterogeneous hypoechoic denoting tendinosis (6)

B- Sonography of calcific tendinitis:

At US, rotator cuff calcifications appear as echogenic foci within the substance of the tendon itself, away from the greater tuberosity. US is excellent in identifying, quantifying and localizing calcium deposits in the rotator cuff. Because of its structure or size, three types of calcifications can be identified with ultrasonography:

- (1) A hyperechoic focus with a well-defined acoustic shadowing (79%).
- (2) A hyperechoic focus with a faint shadow (14%).
- (3) A hyperechoic focus with no shadow (7%).



(4).

Figure (4): Longitudinal and short-axis views of the subscapularis reveal well-defined echogenic foci (*) with posterior acoustic shadowing seen in subscapularis tendon denoting calcific tendinitis (4).

C- Sonographic findings of supraspinatus tendon tears:

Sonographic findings of full-thickness tears (FTT):

When a full-thickness rotator cuff tear occurs, it results in a defect by a variable degree of retraction of the torn tendon ends. The sonographic appearance differs according to the degree of retraction and the amount of fluid filling the resultant defect. Full-thickness rotator cuff tears usually appear as hypoechoic or anechoic defects in which fluid has replaced the area of the torn tendon. Fluid in the region of the torn tendon can also allow increased through-transmission of the ultrasound beam, accentuating the appearance of the underlying cartilage. Thus, two hyperechoic lines

representing the cartilage and the cortex are seen, producing the “double cortex” or “cartilage interface” sign (7).

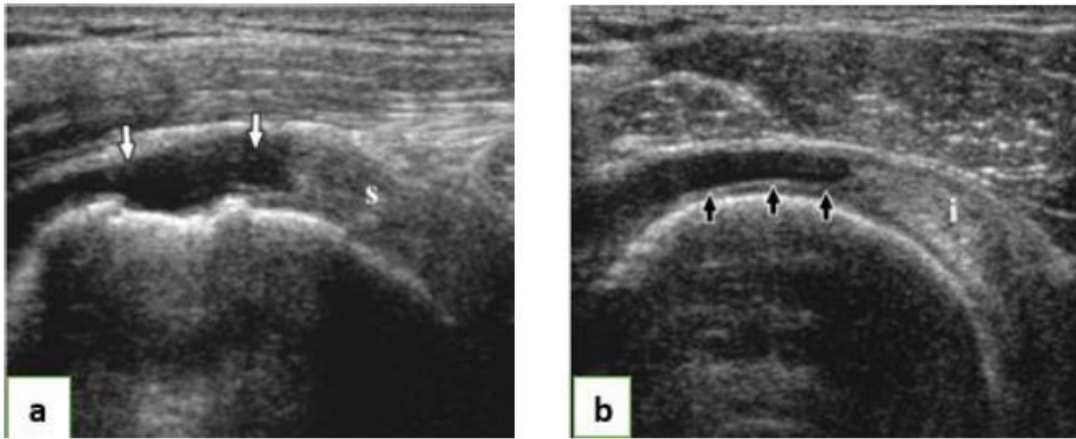


Figure (5): Full-thickness tear of the supraspinatus tendon

(a) Longitudinal US image demonstrates a full-thickness hypoechoic defect in the normal location of the supraspinatus tendon (arrows). This defect represents fluid and extends from the bursal surface to the articular surface. Note the torn edge of the retracted supraspinatus tendon (S).

(b) Transverse US image shows an intact infrapinatus tendon (i) posterior to the tear. The double cortex sign can also be seen; the overlying fluid accentuates the appearance of the cartilage (arrows), which is almost as hyperechoic as the underlying cortex.

(7).

Furthermore, compression over the focal hypoechoic defect will displace the fluid and produce loss of the normal convex contour of the peribursal fat. Loss of normal contour may be seen even without compression if there is no fluid present in the area of the torn and retracted tendon. In this situation, depression of the overlying hyperechoic peribursal fat into the tendon gap occurs, creating the “sagging peribursal fat” sign (7).

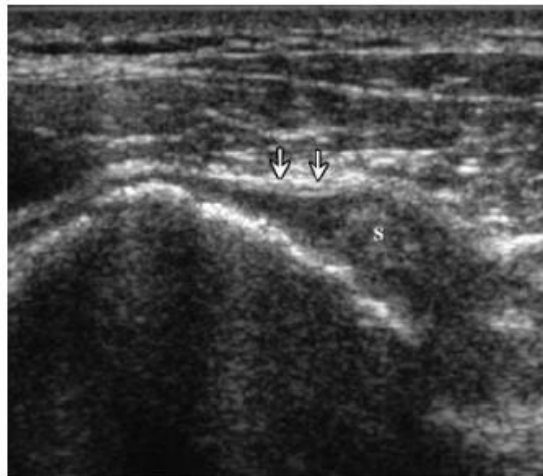


Figure (6): Sagging peribursal fat sign. Longitudinal US image shows a mildly retracted tear of the supraspinatus tendon (S), with sagging of the overlying hyperechoic peribursal fat (arrows) (7).

Sonographic findings of partial-thickness tear (PTT):

Partial-thickness tears occur in a slightly younger age group (30 to 50 years) than full thickness tears. A partial-thickness tear usually occurs along the deep articular side of the rotator cuff and can be recognized as a focal, well-defined hypoechoic or anechoic defect in the tendon which should be visualized in two orthogonal imaging planes to confirm the finding. This should be distinguished from anisotropic effect, which produces less defined hypo echogenicity. Partial-thickness tears may also occur at the bursal side of the cuff or within the substance of the tendon and appear on US as a subtle, focal bursal side defect or an intra tendinous anechoic defect, respectively. Cortical pitting and irregularity can also be seen with partial-thickness tears (7).

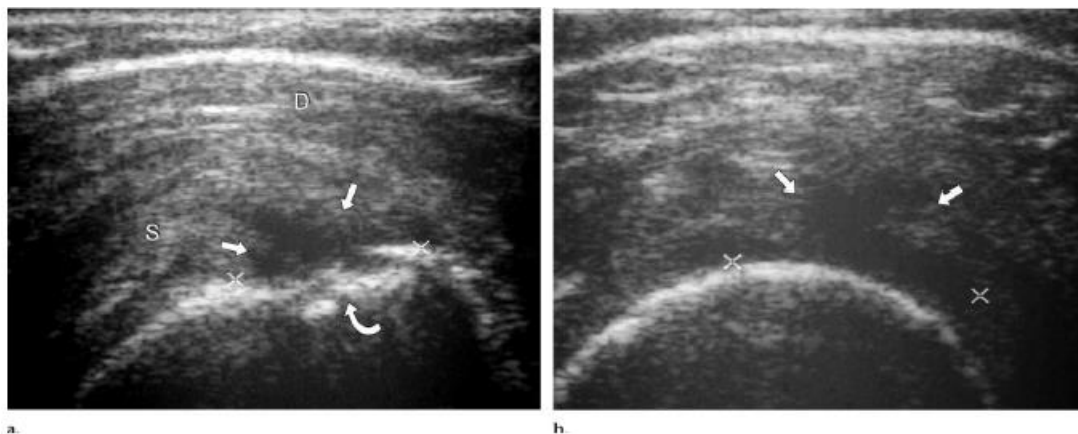


Figure (7): Articular side partial-thickness supraspinatus tendon tear. (a) Longitudinal and (b) transverse US images of the supraspinatus tendon show focal, well-defined anechoic disruption (between cursors and straight arrows) at the distal articular surface of the supraspinatus tendon (S). Note cortical irregularity (curved arrow) of the greater tuberosity. D: deltoid (7).

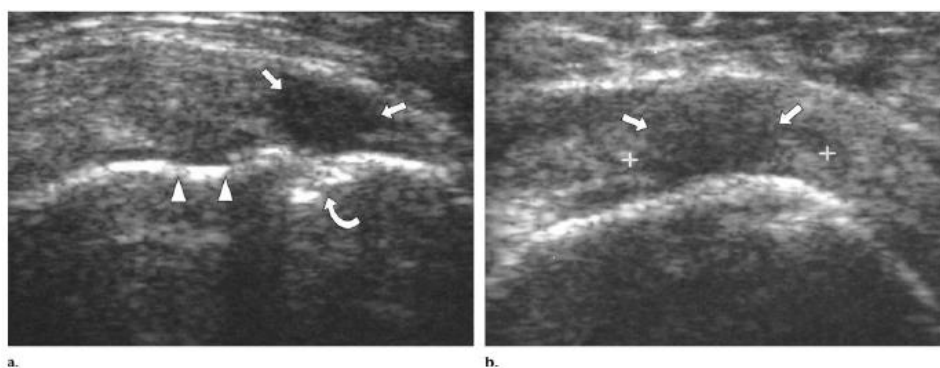


Figure (8): Bursal side partial-thickness supraspinatus tendon tear. US images (a) longitudinal and (b) transverse to the supraspinatus tendon show focal, well-defined anechoic disruption (between cursors and straight arrows) of the distal bursal surface of the supraspinatus tendon. The tendon abnormality extends to the greater tuberosity but does not extend to the articular surface (arrowheads). Note cortical irregularity (curved arrow) of the greater tuberosity (7).

Dynamic sonography:

Dynamic assessment of the rotator cuff and surrounding structures can be performed with ultrasound. Dynamic imaging signs that have been associated with subacromial impingement include lack of convexity of the supraspinatus tendon on its subacromial part, pooling of subacromial bursal fluid in the lateral side of the bursa or increased thickness or buckling of the bursa against the acromion or the CAL during arm abduction (8).

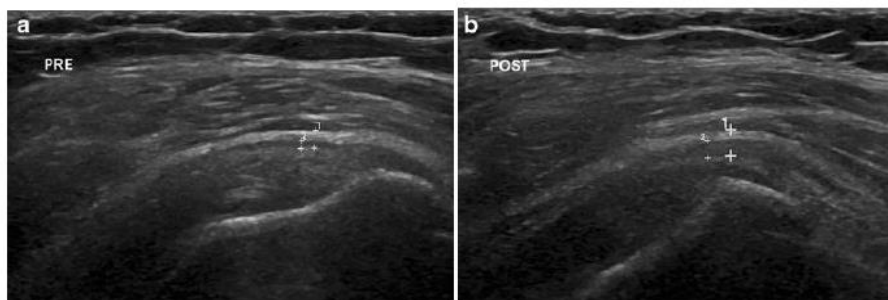


Figure (9): US Images taken (a) before and (b) after dynamic shoulder abduction in a patient with a clinical diagnosis of shoulder impingement. There is increased thickness or “gathering” of the bursal fluid with abduction (9).

Magnetic resonance imaging findings in shoulder impingement syndrome

MRI is the best imaging test prior to arthroscopic surgery. Advantages include the following:

- Noninvasive.
- No radiation.
- Able to detect intrasubstance tendon degeneration or partial rotator cuff tears.
- Able to detect inflammation, edema, hemorrhage, or scarring.
- Able to be used with an intra-articular contrast agent (eg, gadolinium), improving the MRI ability to detect partial rotator cuff tears.

Disadvantages include the following:

- Not able to accommodate patients with claustrophobia.
- Not able to accommodate patients with pacemakers or other metal implants or particles.
- Dependent on quality of the MRI machine.
- Dependent on skill of technician performing the imaging and the radiologist interpreting the images.
- Expensive.

(10)

MRI osseous findings:

Acromial morphology is implicated in the pathogenesis of subacromial impingement. Type III and, to a lesser extent, type II acromion are associated with increased incidence and severity of cuff tears. Both are associated with subacromial spurs and can be evaluated on oblique sagittal MRI (11)



Figure (10): Sagittal T1-weighted fat-saturated MR arthrography image in patient with external subacromial impingement shows type III acromion (*white arrow*) with full thickness rotator cuff tear (*black arrow*) (11) Osacromiale can also be a substrate for impingement. It is important to identify the osacromiale preoperatively, which is best done on the most superior sections of the axial MRI (12)



Figure (11): Osacromiale. Axial T2-weighted MR image through the acromioclavicular joint demonstrates osacromiale (*arrow*) and clavicle (C) (12)

The acromioclavicular joint is the site of degenerative lesions associated with peripheral osteophytes and hypertrophy of the joint capsule. MRI is useful for describing the presence of subchondral edema at the joint edges as well as the presence of a joint effusion. The development of osteophytes at the undersurface of the joint can reduce the subacromial

space and cause subacromial impingement. A laterally or anterior downsloping acromion and a low-lying acromion may also narrow the supraspinatus outlet (13).

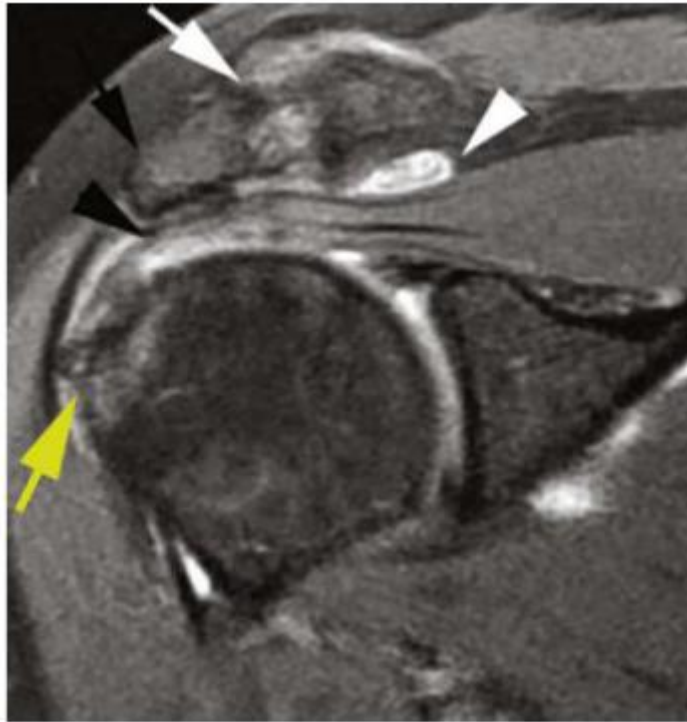


Figure (12): Coronal proton density-weighted fat-saturated MR image in a patient with subacromial impingement demonstrates ACJ degenerative changes (*white arrow*), low-lying acromion with a slight lateral tilt (*black arrow*), subacromial bursitis (*white arrowhead*), partial thickness supraspinatus tear (*black arrowhead*) and changes in the greater tuberosity (*yellow arrow*) (11)

MRI findings of supraspinatus tendon abnormalities:

MRI findings of tendinosis:

Tendinosis of a rotator cuff tendon, a finding frequently present in the anterior portion of the supraspinatus tendon near the insertion at the greater tuberosity, is the initial finding in subacromial impingement. When a tendon demonstrates focal or diffuse regions of intermediate signal intensity, this can be indicative of tendinosis, particularly when the finding is associated with thickening (14)

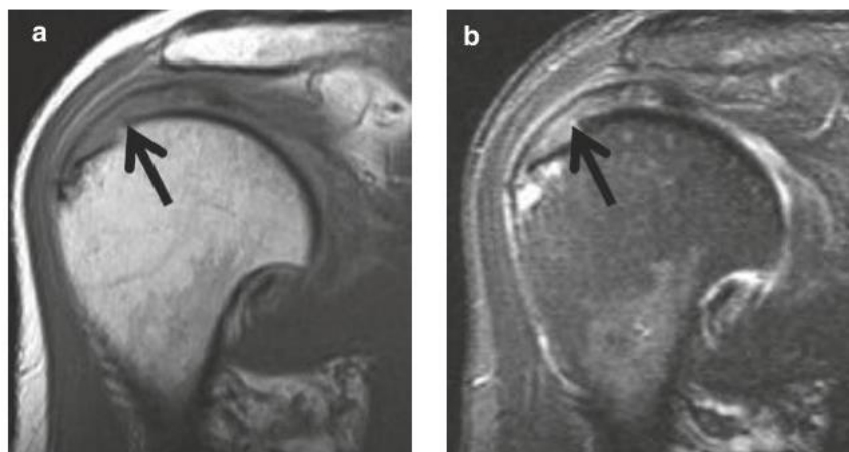


Figure (13): Coronal oblique proton density images (a) without and (b) with fat suppression demonstrate thickening and intermediate signal intensity of the insertional supraspinatus tendon fibers (*arrows*). No discontinuous fibers are seen. The findings are compatible with moderate-severe tendinosis (14)

Partial-thickness tear (PTT) of the rotator cuff:

Partial-thickness tears of the rotator cuff can be diagnosed when there is signal abnormality, approaching the signal intensity of the fluid, extending to the articular or bursal surfaces or within the tendon substance. Articular surface tears are the most common type of partial-thickness rotator cuff tears (14)

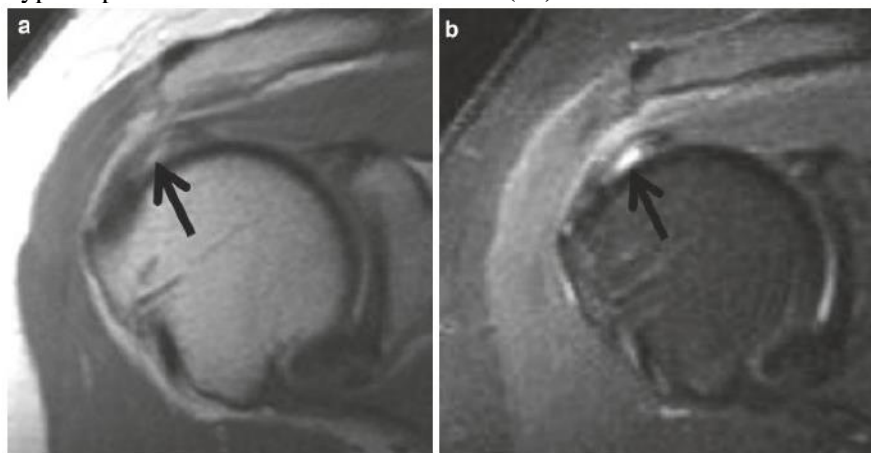


Figure (14): Coronal oblique proton density images (a) without and (b) with fat suppression demonstrates a focal defect with fluid bright signal at the articular surface of the supraspinatus insertion (arrows) compatible with an articular surface partial-thickness tear (14)

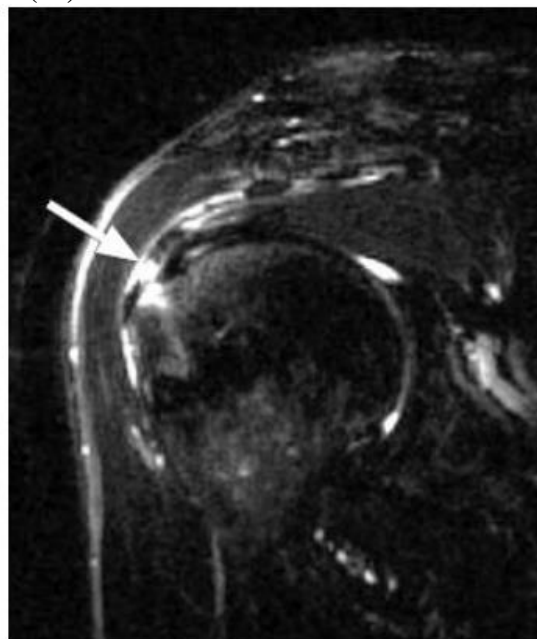


Figure (15): Coronal oblique fat-suppressed T2-weighted MR image shows partial tear of the supraspinatus tendon at bursal surface, outlined by fluid signal, denoting bursal surface partial thickness tear with bone marrow edema at the fibroosseous junction at the greater tuberosity (14)

Increased linear fluid-signal intensity that is located in the mid-layer of the tendon and extends parallel to the long axis of the tendon can represent a partial-thickness intrasubstance tear (15).

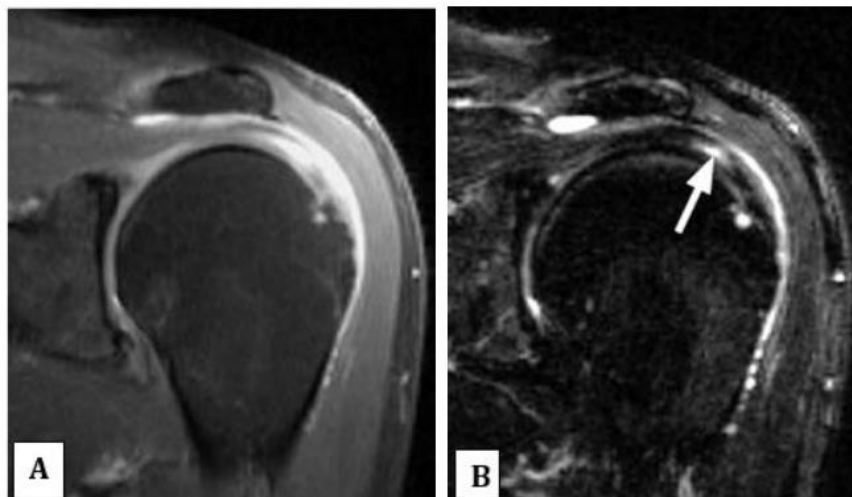


Figure (16): A partial defect in the mid-substance of the supraspinatus tendon with fluid signal is seen well on both the proton-density fat-suppressed image (A) and the STIR image (B) denoting partial thickness intrasubstance tear. There is also a small cyst present in the greater tuberosity at the fibro-osseous junction of the supraspinatus tendon (16).

Full-thickness tear of the rotator cuff:

The diagnosis of a complete or full-thickness tear of a rotator cuff tendon is made with the visualization of a complete defect in the tendon, involving all fibers of the tendon extending from the articular surface to the bursal surface, most commonly involving the supraspinatus tendon. A full thickness tear always creates a communication between the joint cavity and the subacromial bursa (16).



Figure (17): Full-thickness tear of the supraspinatus tendon. Coronal oblique fat-suppressed T2-weighted MR image shows the full-thickness fluid-filled defect (arrows) and the torn retracted edge of the supraspinatus tendon (S) (16).

In the presence of a full thickness tear, especially larger tears, tendon retraction may be present, and the supraspinatus may take on a more globular configuration. Retraction of the torn tendon fibers is best seen on coronal oblique images that demonstrate the medial and lateral extension of the cuff tear. In large to massive tears, the tendon may retract as far as the medial glenoid margin (17).

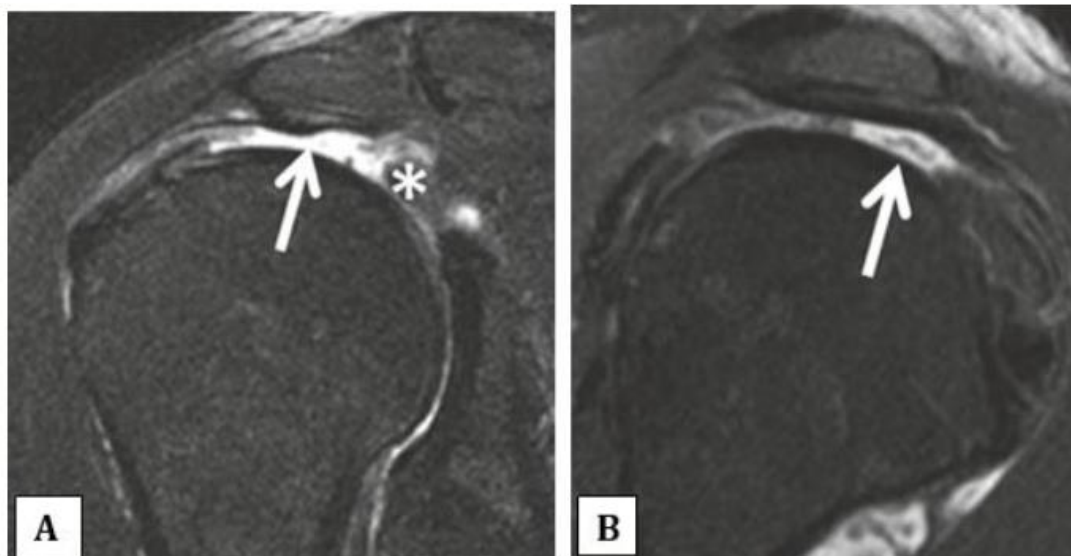


Figure (18): Full-thickness tendon tear

(A) Coronal oblique proton density with fat suppression.

(B) sagittal oblique T2-weighted fat-suppressed images on a patient with a complete tear of the supraspinatus tendon (arrows) evidenced by a full-thickness fluid-filled defect and discontinuity of the tendon. The torn tendon fibers are retracted to the level of the glenoid (asterisk).

(14)

References

1. Garving C, Jakob S, Bauer I, Nadjar R, Brunner UH (2017): Impingement Syndrome of the Shoulder. *DtschArzteblInt*; 114(45): 765-776.
2. Kadi R, Milants A, Shahabpour M (2017): Shoulder Anatomy and Normal Variants. *J Belg Soc Radiol*; 101(Suppl 2): 3.
3. Hauser-Bischof, C (2003): *Schulterrehabilitation in der Orthopädie und Traumatologie*. Thieme Verlag, Stuttgart; 19.
4. Singh, R., Narayan, S., Verma, V., and Rai, V. (2016): Spectrum of high resolution sonographic findings in painful shoulder. *Astrocyte*; 2(4): 200.
5. Yemin, A., and Adler, R. S. (2019): Sonographic Evaluation of the Shoulder. In: *The Shoulder*. Springer; 55-65.
6. Ivanoski, S. (2014): Ultrasound assessment of most frequent shoulder disorders.
7. Moosikasowan, J. B., Miller, T. T., and Burke, B. J. (2005): Rotator cuff tears: Clinical, radiographic, and US findings. *Radiographics*; 25(6): 1591-1607.
8. Chang, E. Y., and Chung, C. B. (2019): Imaging Diagnosis of Rotator Cuff Pathology and Impingement Syndromes. In *The Shoulder*. Springer; 87-125.
9. Dagher, A. A., Sookur, P. A., Shah, S., and Watson, M. (2012): Dynamic ultrasound of the subacromial-subdeltoid bursa in patients with shoulder impingement: A comparison with normal volunteers. *Skeletal Radiology*; 41(9): 1047-1053.
10. Lewis JS. (2008): Rotator cuff tendinopathy / subacromial impingement syndrome: Is it time for a new method of assessment? *British Journal of sports Medicine*; 43 (4): 259-64.
11. Mulyadi, E., Harish, S., O'Neill, J., and Rebello, R. (2009): MRI of impingement syndromes of the shoulder. *Clinical Radiology*; 64(3): 307-318.
12. Cook, T. S., Stein, J. M., Simonson, S., and Kim, W. (2011): Normal and Variant Anatomy of the Shoulder on MRI. *Magnetic Resonance Imaging Clinics of North America*; 19(3): 581-594.
13. Pesquer, L., Borghol, S., Meyer, P., Ropars, M., Dallaudière, B., & Abadie, P. (2018): Multimodality

imaging of subacromial impingement syndrome. *Skeletal Radiology*; 47(7): 923–937.

- 14.** Meraj, S., and Bencardino, J. T. (2019): Technical Update in Conventional and Arthrographic MRI of the Shoulder. In *The Shoulder*. Springer; 23–54.
- 15.** Mesiha, M. M., Derwin, K. A., Sibole, S. C., Erdemir, A., & McCarron, J. A. (2013): The biomechanical relevance of anterior rotator cuff cable tears in a cadaveric shoulder model. *JBJS*; 95(20): 1817–1824.
- 16.** Davies, A. M., and Hodler, J. (2006): *Imaging of the Shoulder*. Springer.
- 17.** Zlatkin, M. B. (2003): *MRI of the shoulder*. Lippincott Williams & Wilkins.